Molecular Cell, Vol. 11, 79–90, January, 2003, Copyright ©2003 by Cell Press

N-Linked Glycans Direct the Cotranslational Folding Pathway of *Influenza* Hemagglutinin

Robert Daniels,[1] Brad Kurowski,[1] Arthur E. Johnson,[2] and Daniel N. Hebert[1,*]
[1]Department of Biochemistry and Molecular Biology
Program in Molecular and Cellular Biology
University of Massachusetts
Amherst, Massachusetts 01003
[2]Department of Medical Biochemistry and Genetics,
Department of Chemistry, and
Department of Biochemistry and Biophysics
Texas A&M University System Health Sciences Center
College Station, Texas 77843

Summary

For proteins that traverse the secretory pathway, folding commences cotranslationally upon translocation into the endoplasmic reticulum. In this study, we have comprehensively analyzed the earliest maturation steps of the model glycoprotein *influenza* hemagglutinin (HA). These steps include cleavage of the signal sequence, glycosylation, binding by the chaperones calnexin and calreticulin, and the oxidoreductase ERp57, and oxidation. Our results show that the molecular choreography of the nascent HA chain is largely directed by multiple glycans that are strategically placed to elicit the binding of lectin chaperones. These chaperones are recruited to specific nascent chain locations to regulate and facilitate glycoprotein folding, thereby suggesting that the positioning of N-linked glycans in critical regions has evolved to optimize the folding process in the cell.

Introduction

Protein folding occurs through multiple pathways by progressively restricting the conformations available to a polypeptide chain until the native structure is reached. For longer multidomain proteins, an enormous number of conformations are available, and the folding reaction frequently culminates in misfolded, kinetically trapped, or aggregated products. The folding of complex proteins in the crowded confines of the cell at biological temperatures would appear to be an insurmountable task, yet proteins routinely fold rapidly and efficiently under these conditions. Understanding the cellular environment where folding occurs and the mechanisms that enable proteins to acquire their native structures with high fidelity are critical goals.

Recent studies have demonstrated that cotranslational folding occurs in both the cytosol and the endoplasmic reticulum (ER), the site of folding for proteins that traverse the secretory pathway. Cytosolic proteins can bind chaperones and obtain protease-resistant conformations while associated with ribosomes (Netzer and Hartl, 1997; Frydman et al., 1999). Most strikingly, the Semliki Forest virus (SFV) capsid protein can exhibit its autocatalytic proteolytic activity in both eukaryotic cells and prokaryotic spheroplasts while still bound to the ribosome (Nicola et al., 1999). For viral proteins that enter the ER, including the *influenza* hemagglutinin (HA) protein and SFV glycoproteins, disulfide bond formation and chaperone binding commence cotranslationally (Chen et al., 1995; Hebert et al., 1997; Molinari and Helenius, 1999). The ER translocon itself has been shown to assist in the maturation process by providing a protective environment that inhibits protein aggregation (Chen and Helenius, 2000), yet the organization of the translocon and translocon-associated proteins that are responsible for this assistance remain poorly understood.

The cotranslational processing of secretory proteins also includes the removal of N-terminal signal sequences and the transfer and trimming of N-linked glycans. Once an Asn in the glycosylation consensus sequence of Asn-X-Thr/Ser is extended ~11 amino acids into the lumen, it can receive a 14-member sugar moiety en bloc (Whitley et al., 1996). Two glucoses of this modification are then rapidly and sequentially removed by glucosidases I and II, creating a monoglucosylated protein. This monoglucosylated glycan is a substrate for calnexin (CNX) and/or calreticulin (CRT), homologous lectin chaperones of the ER (Hammond et al., 1994). When the final glucose is removed by glucosidase II, neither CNX nor CRT is able to bind to the nascent chain. Rebinding to the chaperone can be reinitiated by the transfer of glucose to a misfolded or unassembled protein by the UDP-glucose: glycoprotein glucosyltransferase (UGT) (Helenius, 1994; Sousa and Parodi, 1995). During this process, ERp57, a protein disulfide isomerase (PDI) family member of the ER, may act as an oxidoreductase, assisting in the formation and isomerization of disulfide bonds (Zapun et al., 1998; Oliver et al., 1999). Therefore, the maturation and quality control processes of glycoproteins in the early secretory pathway rely on CNX, CRT, ERp57, and UGT for proper function (Ellgaard et al., 1999).

The earliest steps in the folding process are critical for obtaining a native structure in vitro. In the cell, protein folding begins during synthesis (cotranslationally), thereby permitting separate domains of a polypeptide to fold independently. Temporal and spatial separation of the folding of individual domains in a multidomain protein limits the total number of available conformations that can be sampled. Therefore, a vectorial folding process, with domains folded sequentially as they emerge from the biosynthetic and translocation machinery, could potentially direct the more efficient folding of proteins and control access to the nascent protein when it is most susceptible to being diverted down an incorrect folding pathway (Hardesty et al., 1999).

The maturation of HA has been extensively studied in *influenza*-infected cells and with a cell-free system (Braakman et al., 1992; Hebert et al., 1995), making it a paradigm for understanding the maturation and quality control processes of the secretory pathway. Both CNX and CRT bind HA cotranslationally (Chen et al., 1995; Hebert et al., 1997); however, the sequence of events

*Correspondence: dhebert@biochem.umass.edu

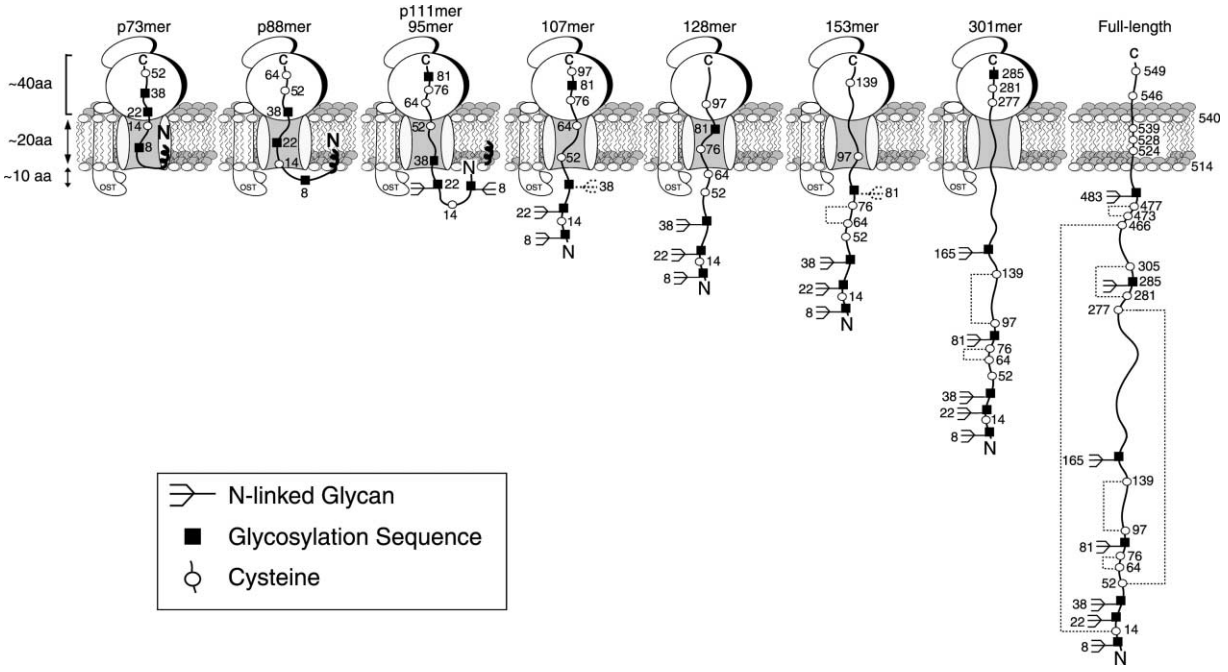

Figure 1. The Topology of Ribosome-Bound HA Chains

The diagram displays the ~70 residues bridging the ribosomal P site to the OST active site (Whitley et al., 1996), and the Cys residues (circles) and N-linked glycans (branched structure) for each polypeptide. The native disulfide bonds and the sites that are only partially glycosylated are designated by dashed lines and branched structures, respectively.

during the critical initial stage of the maturation pathway is not known because the protein was visualized only after ~30% of it had been translated. Here, we used truncated ribosome-bound nascent chains combined with ER-derived microsomes, a system that has previously been employed to identify ER translocon components (Krieg et al., 1989; Gilmore et al., 1991), to accumulate translocation intermediates. The cotranslational maturation process of HA was characterized, and the translocon-associated proteins involved in ensuring that maturation proceeds accurately were identified.

Results

Translocation and Glycosylation of Ribosome-Attached Proteins

HA is a type I membrane glycoprotein with seven N-linked glycosylation sites and six disulfide bonds (Figure 1). To examine the cotranslational folding process of HA and probe the environment of the nascent HA chain during passage through the translocon and into the ER lumen, translationally arrested HA chains of increasing lengths were generated. This was accomplished by translating truncated mRNAs that lacked a stop codon, thereby yielding translation intermediates in which the length of the nascent chain is dictated by the length of the truncated mRNA (Krieg et al., 1989; Gilmore et al., 1991).

To characterize the modifications to HA at different stages of its translation, full-length and truncated mRNAs were translated in the absence or presence of microsomes. Seven truncated proteins termed X-mers (X equals the number of amino acids of the mature protein) or pX-mers (X equals the number of amino acids in the preprotein including the 16 residue signal sequence), as well as the full-length HA, were synthesized and resolved by SDS-PAGE (Figure 2A). Proteins translocated into ER microsomes increased in molecular weight due to the addition of N-linked carbohydrates (2.5 kDa/carbohydrate), with the exception of the p73-mer and p88-mer, where the first consensus glycosylation site is unable to reach the oligosaccharyltransferase (OST) active site (Figure 2A, lanes 1–4). The distance between the ribosomal P site and the OST active site is ~70 amino acids (Whitley et al., 1996). Therefore, a nascent protein must have a minimum of 70 amino acids added after the glycosylation sequence for it to receive the N-linked carbohydrate (Figure 1). For example, the translocated 128-mer is resolved as a single band with three carbohydrates at Asn8, 22, and 38 because Asn81 has not yet reached the OST active site (Figure 2A, lane 10).

In contrast to the 128-mer, a protein doublet with an approximate molecular weight difference of one glycan was observed for the microsome-translocated 95-, 107-, and 153-mers (Figure 2A, lanes 6, 8, and 12, filled circles). To determine the corresponding number of glycans added to the constructs and, more specifically, whether the doublets arose from partial glycosylation of N-linked consensus sites, ribosome-bound and puromycin-released forms of HA were analyzed. For the 95-mer, ribosome-release of nascent chains by puromycin permitted the partial recognition of two consensus glycosylation sites that were sequestered within the ribosome and translocon (Figure 1). Thus, five bands were observed corresponding to the unglycosylated form (Figure 2B, lanes 1 and 2, band designated "0") and proteins with one, two, three, or four glycans transferred

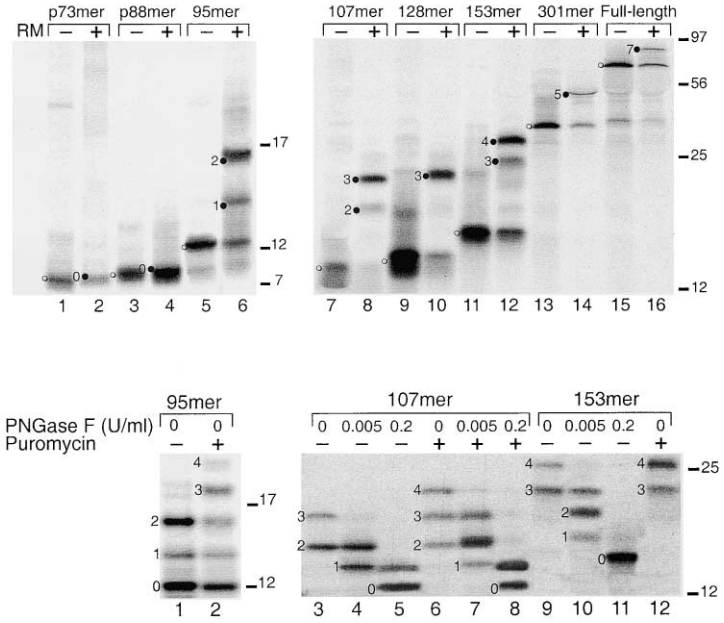

Figure 2. Monitoring the ER Targeting and Ribosomal Release of HA Nascent Proteins

(A) Radiolabeled chains of increasing lengths were synthesized in the presence or absence of rough microsomes (RM) and then immunoprecipitated with HA antisera. Samples 1–6 and 7–16 were analyzed by 14% Tris-tricine-PAGE and 5%–20% SDS-PAGE, respectively, followed by autoradiography. Closed circles show translocated and glycosylated chains with the number of glycans indicated. Open circles indicate untranslocated HA. Six Met were substituted into the ribosome/translocon complex of the six shortest truncations to increase the number of ^{35}S-labeled residues and minimize their effects on lumenal interactions.

(B) HA transcripts were translated and then released from the ribosome with puromycin (lanes 2, 6–8, and 12). After translation, the arrested chain and the released 107- and 153-mer constructs were digested with the indicated concentrations of PNGase F and immunoprecipitated with HA antisera.

(designated "1–4"). Therefore, the ribosome-bound protein triplet with the 95-mer (Figure 2A) corresponded to polypeptides with zero, one, or two glycans.

The complete glycosylation status of the longer constructs could not be determined by puromycin release. Instead, these samples were exposed to varying concentrations of the endoglycosidase F (PNGase F) after microsome lysis allowing all stages of glycosylation or "rungs of the glycan ladder" to be observed, enabling the total number of glycans to be determined. The 107-mer possessed a maximum of three glycans in its ribosome-bound form (Figure 2B, lanes 3–5), while the puromycin-released form had four glycans (Figure 2B, lanes 6–8). The 107-mer doublet (Figure 2A, lane 8; Figure 2B, lane 3) was a result of partial glycosylation of Asn38, located ~70 amino acids from the ribosomal P site and hence close to the OST active site. Upon puromycin release of the nascent chain, inefficient glycosylation at Asn81 yielded another glycosylated nascent chain with four glycans transferred (Figure 2B, lane 6). Based on the ~70 residue minimum for glycosylation and the molecular weight shifts due to glycosylation, the glycosylation status of each construct was determined as indicated in Table 1 (also denoted in Figure 2A).

Though mRNAs lacking a stop codon yield translationally arrested proteins, time-dependent release from the ribosome can occur. A 30 min translation was determined to yield the optimum fraction of ribosome-bound arrested chains (data not shown). Therefore, this time was used for all subsequent experiments.

Signal Sequence Cleavage Commences with the p111-mer

The hydrophobic N-terminal signal sequence of HA has been proposed to play a key role in the folding process by helping to position the N terminus proximal to the membrane, its position in its mature form (Wilson et al., 1981). To understand the role that the signal sequence may play in the folding of HA, the timing of the signal sequence removal was determined using two methods. One method monitored the loss of radioactive label in the signal sequence, while the second utilized an antibody that recognizes HA after its signal sequence has been cleaved.

For HA, the single initiator Met is the only Met until position 168. Therefore, nascent chains shorter than 168 amino acids and labeled with [^{35}S]Met can only be detected if the signal sequence is present. Since both the p73-mer and p88-mer are visible by SDS-PAGE, they each retained their signal sequence (Figure 3A, lanes 1 and 3). In contrast, the 107-, 128-, and 153-mers were not detected, showing that they all existed in the mature signal sequence-cleaved form (Figure 3A, lanes 7, 9, and 11). To ensure that each HA construct had efficiently translated, a parallel experiment was performed using both [^{35}S]Met and [^{35}S]Cys, since a large number of Cys residues are located at the N terminus of HA. Interestingly, the lower band of the 95-mer doublet corresponding to the addition of a single glycan primarily at Asn8 (data not shown) was present with [^{35}S]Met labeling, while the twice-glycosylated form was not (Figure 3A, lane 5). This indicated that the p111-mer was partially cleaved and that the cleaved form was more efficiently glycosylated at Asn22, presumably because of the increased freedom of the polypeptide after release from the membrane-anchoring signal sequence.

To verify that signal sequence cleavage commenced with the p111/95-mer, a polyclonal antibody (α-HA N-T) was used that recognized HA only after its signal sequence is cleaved. This antibody was raised against a peptide consisting of the 12 N-terminal residues of the mature (signal sequence-cleaved) form of HA (Figure 3B), and it immunoprecipitated this form, but not HA that had retained its signal sequence. HA nascent chains of different lengths were immunoprecipitated with the

Table 1. Characteristics of HA Ribosome-Bound and Released Chains

Amino Acid Residues	Number of Glycans: Ribosome-Bound	Number of Glycans: Ribosome-Released	Molecular Mass (kDa): − Microsomes[c]	Molecular Mass (kDa): Translocated: Bound	Molecular Mass (kDa): Translocated: Released	Met/Cys
p73	0	1	7.8	7.8[c]	10.3	6/3[b]
p88	0	1	9.3	9.3[c]	11.8	6/4[b]
p111	1	2	12	14.5[c]	17	6/5[b]
95	2	3	12	15.3	17.8	6/5[b]
107	2/3	4	13.4	16.7/19.2	21.7	6/5[b]
128	3	4	15.7	21.5	24	6/5[b]
153	3/4	4	18.4	23.2/25.7	25.7	6/6[b]
301	5	6	34.8	45.5	48.0	3/8
551[a]	NA	7	63.4	NA	79.2	8/17

[a] Full-length.
[b] Proteins that contain six added Met to enhance detection.
[c] The − Microsomes molecular mass includes the 1.8 kDa signal sequence.

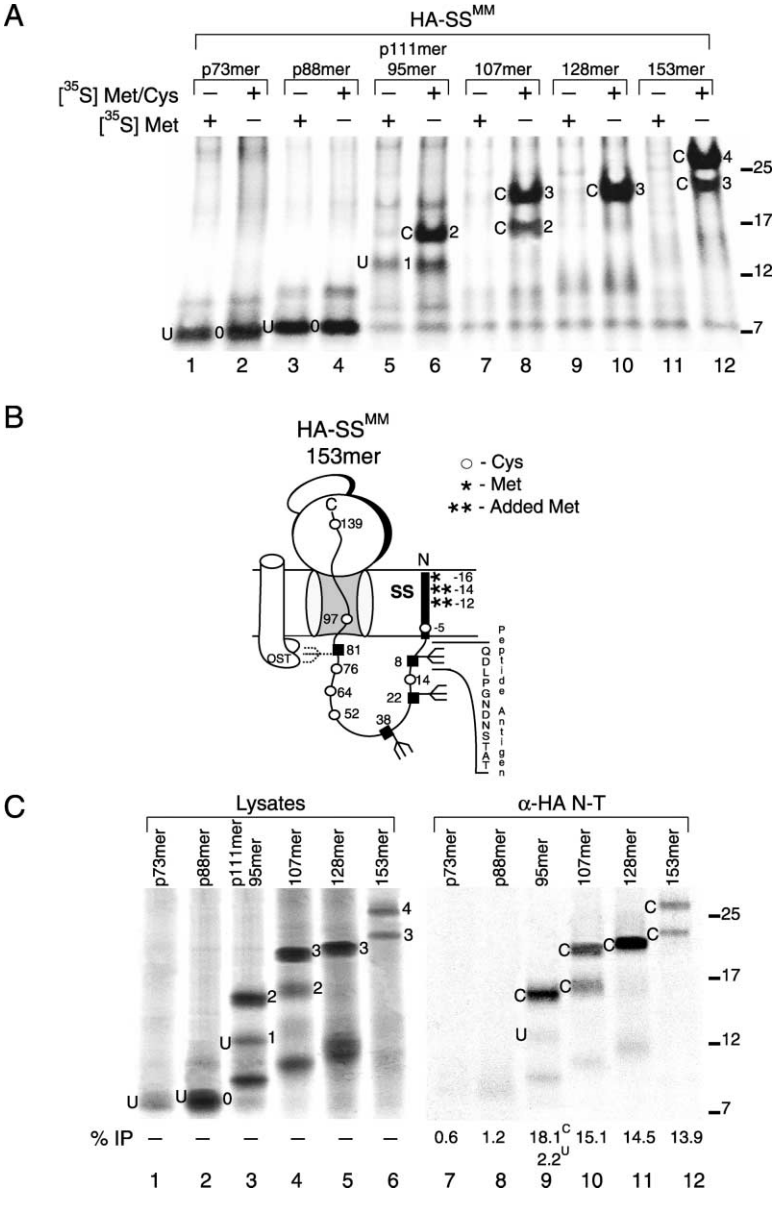

Figure 3. HA Signal Sequence Cleavage Commences with the p111-mer

(A) HA transcripts were translated using a construct with two Met residues substituted at positions −14 and −12 in the signal sequence to enhance detection. Translations were performed with [35S]Met to visualize only the uncleaved constructs, while both [35S]Met and [35S]Cys were used to visualize all translation products. Translation products were precipitated by CTAB to isolate only those nascent chains still attached to a tRNA prior to analysis by 14% Tris-tricine-PAGE. The cleaved ("C") and uncleaved ("U") products, and glycan numbers are designated.

(B) The cartoon of the 153-mer indicates the Met substitutions in (A) and the peptide antigen of HA N-terminal antibody (α-HA N-T) used in (C).

(C) The p73-mer up to the 153-mer with wild-type signal sequence was translated. Lysates were examined directly (lanes 1–6) or immunoprecipitated with α-HA N-T (lanes 7–12) prior to analysis by 14% Tris-tricine-PAGE. The percent of each construct immunoprecipitated was calculated as listed at the bottom of the autorad.

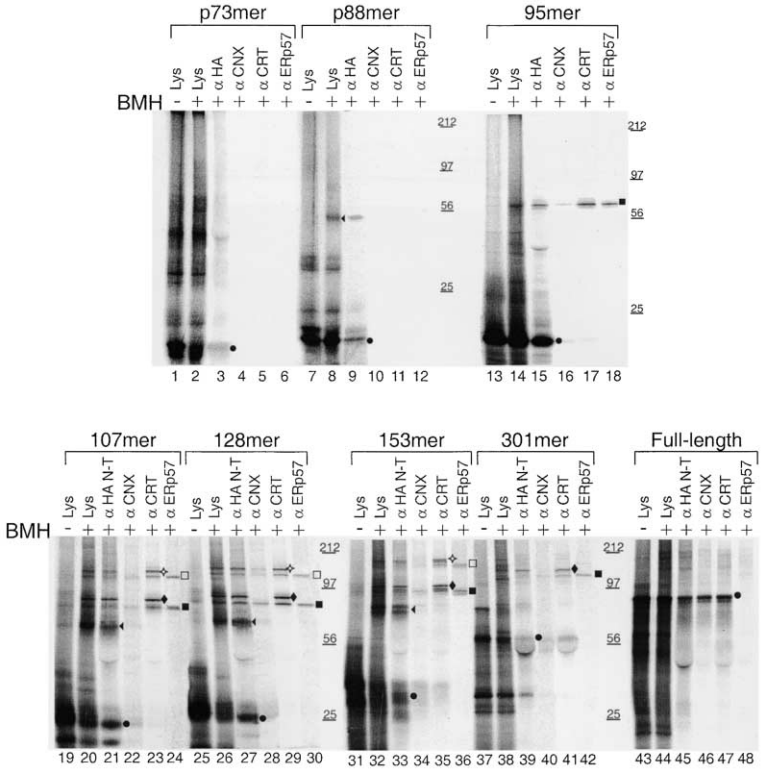

Figure 4. The Cotranslational Translocation of HA into the ER, Followed by Crosslinking

HA chains of increasing length were translated and subjected to crosslinking with bismaleimidohexane (BMH) as indicated. Lysate ("Lys"), and samples immunoprecipitated under native conditions with HA, CNX, CRT, and ERp57 antibodies are shown as indicated. Samples 1–18 and 19–48 were resolved by 8%–17% and 7.5%–12.5% SDS-PAGE, respectively. Uncrosslinked translocated HA is identified by a solid circle, while HA crosslinks to Sec61α, CRT, and ERp57 are identified by solid arrows, diamonds, and squares, respectively. Ternary complexes of HA, Sec61α, and CRT or HA, Sec61α, and ERp57 are denoted by open stars and squares, respectively.

α-HA N-T antibody to confirm that the slowest migrating 95-mer band with two glycans was the first form of HA to have its signal sequence removed (Figure 3C). Therefore, signal sequence cleavage commenced when the HA nascent chain reached a length near 111 amino acids, and this timing was unaltered when glycan addition or trimming was prevented (data not shown).

Chemical Crosslinking of Nascent Chains to Sec61α, CRT, and ERp57

To examine the environment of the nascent chain as it is translocated through the translocon and emerges into the ER lumen, chemical crosslinking was used to identify which translocon or lumenal proteins were adjacent to the Cys residues in the nascent chain. Translocation intermediates were treated with the thiol-reactive crosslinker bismaleimidohexane (BMH) prior to membrane lysis.

Crosslinking resulted in the formation of a single adduct to the p88-mer and 95-mer, and five adducts to the 107-, 128-, and 153-mers that were resolved by immunoprecipitation with anti-HA antibodies and SDS-PAGE. The covalent partner generated with the p88-mer was ~40 kDa (Figure 4, lane 8, arrowhead), while that with the 95-mer was ~60 kDa (Figure 4, lane 18, solid square). Crosslinked partners produced with the 107-, 128-, and 153-mers all included a 40 kDa protein and two protein doublets of approximately 60 and 100 kDa (Figure 4, lanes 21, 27, and 33). The 301-mer only generated the 60 kDa doublet, while the shortest construct (p73mer) and the full-length protein had no observable crosslinks. The close proximity of the crosslinked partners to HA was confirmed by crosslink formation after high levels of oxidized glutathione or diamide were added posttranslationally (data not shown).

To identify the crosslinking partners, crosslinked ^{35}S-labeled HA was immunoprecipitated under native conditions using antisera raised against a variety of ER resident proteins, including BiP, CNX, CRT, ERp57, GRP94, and PDI. From this group, adducts were immunoprecipitated with CNX, CRT, and ERp57 antisera (Figure 4, and data not shown). Specifically, the single crosslink (60 kDa) to the 95-mer (square) and the lower band of each of the protein doublets (60 and 100 kDa) found on the 107-, 128-, and 153-mers were immunoprecipitated with anti-CRT and anti-ERp57 sera and weakly with CNX antisera. The upper bands of the doublets were precipitated only by CRT antisera (diamonds). The 301-mer 60 kDa doublet had similar characteristics to those observed for the 107-, 128-, and 153-mers, with the lower band being immunoprecipitated by anti-CRT and anti-ERp57 sera and the upper band being recognized solely by anti-CRT sera (Figure 4, lanes 39–42).

Since CNX and CRT binding to carbohydrates can survive the native immunoprecipitation procedures, the crosslinks are immunoprecipitated with multiple antibodies because the HA nascent chains are simultaneously associated with multiple proteins (e.g., the 60 kDa crosslink in Figure 4, lanes 27–30). Thus, the same experiment was performed under denaturing conditions (data not shown). Binding to CNX was completely disrupted, but anti-CRT continued to immunoprecipitate both pairs of protein doublets of 60 and 100 kDa. Anti-ERp57 immunoprecipitated only the lower bands of both doublets, so the lower band was a crosslink to ERp57. The larger 60 kDa band therefore results from a HA crosslink to

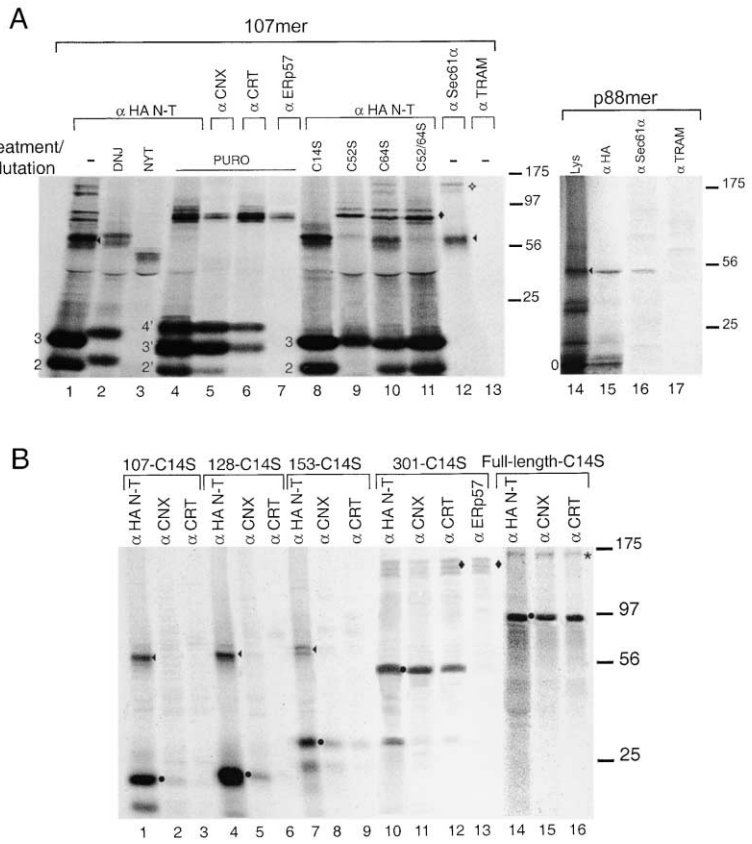

Figure 5. Identification of HA Crosslinking Sites and Targets

(A) The p88-mer and the 107-mer HA arrested chains were crosslinked using BMH. The 107-mer was analyzed using inhibitors of glycosylation trimming (DNJ) or addition (NYT), nascent chain release (PURO), and Cys mutants. Samples were treated with DNJ or NYT prior to translation as indicated. The apostrophes indicate increased glycan trimming that occurs upon puromycin release (data not shown). The p88-mer lysate sample ("Lys") was resolved to show all radioactive species; all other samples were analyzed after immunoprecipitation with anti-HA, anti-Sec61α, or anti-TRAM antibodies under native conditions. All samples were resolved by 9%–17.5% SDS-PAGE. The HA crosslinks to Sec61α and to CRT/ERp57 are shown with triangles and diamonds, respectively. Ternary covalent complexes containing Sec61α/CRT and Sec61α/ERp57 in addition to nascent HA are shown by stars.

(B) HA constructs were mutated at Cys14 to Ser (C14S) and subjected to BMH crosslinking. All samples were immunoprecipitated under native conditions with HA, CNX, CRT, and ERp57 antibodies where indicated prior to resolution by 7.5%–12.5% SDS-PAGE. Translocated HA, or HA polypeptides crosslinked to Sec61α, CRT, ERp57, and an ~80 kDa crosslink are shown by solid circles, triangles, diamonds, and an asterisk, respectively.

CRT, because CRT and ERp57 are both ~60 kDa. Interestingly, anti-CRT also immunoprecipitated the ERp57 crosslink, indicating that the noncovalent CRT-ERp57 interaction was not completely disrupted by the denaturing conditions. The 60 kDa doublet therefore corresponds to 1:1 crosslinks between HA and CRT and between HA and ERp57. As shown below, the 100 kDa doublet then results from an HA nascent chain crosslinking simultaneously to the 40 kDa target protein and to either CRT or ERp57.

To confirm these assignments, we focused on the 107-mer that contained all of the observable crosslinks and had a crosslinking pattern similar to the 128- and 153-mers. First, the 107-mer was translated in the presence of inhibitors that are known to abolish lectin chaperone interactions (Hammond et al., 1994). In the presence of the glucosidase inhibitor n-butyl deoxynojirimycin (DNJ) or the tripeptide NYT that competitively inhibits the OST, only crosslinking to the 40 kDa protein persisted (Figure 5A, lanes 2 and 3).

The inhibitor-mediated disappearance of the 60 and 100 kDa crosslinked-partner doublets verified that these interactions were carbohydrate mediated. Furthermore, the site on HA that supported crosslinking to the lectin chaperones and ERp57 was determined to be Cys14, since these adducts disappeared after mutation of Cys14 to a Ser (Figure 5A, lane 8). Cys14 also supported the crosslinking to CRT and ERp57 for the 128- and 153-mers, even though one and three additional Cys, respectively, had entered the ER lumen (Figure 5B). HA crosslinking to CRT or ERp57 was not observed in the absence of Cys14 until five additional Cys were located in the ER lumen with the 301-mer (Figure 5B, lanes 10–13).

Several lines of evidence indicate that the 40 kDa crosslinking target corresponds to a protein in the translocon pore: (1) it persisted in the presence of inhibitors of carbohydrate transfer or trimming (Figure 5A); (2) it was the only adduct that remained with the 107-mer-C14S mutation that lacked lumenal Cys, but possessed two Cys residues localized in the transmembrane pore of the translocon (Figure 5A, lane 8, and see Figure 1); (3) the adduct was not seen with the 301-mer that does not have a Cys in the translocon pore (Figure 4, lane 39); and (4) the release of the nascent chains with puromycin or the Cys to Ser conversion in the translocon pore ablated the crosslink to the 40 kDa target protein, while crosslinking to the 60 kDa target proteins persisted (Figure 5A, lanes 4 and 11).

To determine the identity of the translocon protein that was crosslinked to the p88-, 107-, 128-, and 153-mers, immunoprecipitations were performed with Sec61α and TRAM antisera, proteins that migrate at ~40 kDa by SDS-PAGE (Figure 5A, lanes 12, 13, 16, and 17). The single 40 kDa crosslink to the p88-mer and both the 40 kDa and 100 kDa doublets found on the 107-mer were immunoprecipitated by Sec61α antisera, demonstrating that Sec61α was present in each of these adducts. Thus, the adduct containing the 40 kDa target protein is a binary complex of Sec61α and HA, while the adduct containing a 100 kDa target protein doublet arises from ternary complexes containing HA, Sec61α, and either

CRT or ERp57. This conclusion was supported by the absence of the 100 kDa species whenever the adduct containing the 40 kDa target protein was not formed.

CNX Binds Initially, Followed by CRT

To examine the temporal binding of lectin ER chaperones to HA nascent chains, the ^{35}S-labeled HA translocation intermediates were translated and immunoprecipitated with CNX or CRT antisera under native conditions. Coimmunoprecipitation of nascent HA with CNX or CRT was not observed for the two shortest constructs or the singly glycosylated p111-mer that still possesses its signal sequence (Figure 6A, lanes 7–12, and Figure 6B). CNX bound the mature 95-mer (p111-mer minus its signal sequence with two glycans present) with ~2% efficiency, but CRT binding was undetectable. CNX binding to the 107-mer increased to ~5% efficiency, and CRT binding remained very weak (Figure 6A, lanes 23 and 28, and Figure 6B). The 128-mer exhibited similar CNX and CRT binding characteristics and bound preferentially to CNX. Since the first three glycans (8, 22, and 38) are present on both the 107- and 128-mers, these glycans supported CNX binding as previously proposed for the full-length protein (Hebert et al., 1997).

With the 153-mer, CNX binding persisted, and CRT binding began to increase slightly after the addition of the glycan at Asn81 that resides in the top domain of HA (Figure 6A, lanes 25 and 30, and Figure 6B). Though minimal CRT binding is seen with the 153-mer, this binding was found to be completely dependent on glycans 38 and 81, as removal of either glycan decreased CRT binding by 50% (data not shown). The efficiency of CRT binding increased to the level of CNX binding with the 301-mer that contained the three stem-domain glycans 8, 22, and 38 as well as the top domain glycans 81 and 165 (Figure 6A, lanes 26 and 31, and Figure 6B). Both CNX and CRT bound the full-length protein that contained seven N-linked glycans. However, CNX binding increased to ~21%, while CRT binding remained at ~13% (Figure 6A, lanes 27 and 32, and Figure 6B). The two additional glycans at Asn285 and 483 on the full-length protein are likely responsible for the observed increase in CNX binding.

Altogether, these results showed that CNX initially binds the shorter ribosome-attached chains that constitute early stages in the cotranslational folding and processing of HA. While crosslinking of HA demonstrates that CRT is in the vicinity, CRT does not bind stably to HA until glycans on the top domain of HA are accessible in the lumen. In contrast, CNX binds HA nascent chains once the appropriate glycan is exposed, with the level of binding ultimately increasing when the sixth and seventh glycans are present on the full-length protein.

Location of HA Dictates the Chaperone Binding Profile

To determine whether the attachment of the HA nascent chain to the ribosome/ER translocon complex determines chaperone binding patterns, proteins were translated and treated with puromycin to release the chain from the ribosome/translocon complex. HA was then coimmunoprecipitated with anti-CNX or anti-CRT sera.

In the absence of puromycin, the 128-mer was observed as a single band corresponding to the translocated protein with three glycans (Figure 6C, lane 1). Upon liberation from the ribosome with puromycin, the 128-mer appeared as a protein doublet, as the fourth glycan at Asn81 is inefficiently recognized during release (Figure 6C, lane 4). The release and additional glycan dramatically changed the binding patterns of CNX and CRT as compared to the ribosome-bound 128-mer. While CNX bound both species, CRT bound only the released forms (Figure 6C, lanes 3 and 6).

To determine if the increase in CRT binding to the released chain was due to its change in location or to the increase in the number of glycans, the 153-mer was examined. The 153-mer possessed four glycans in its ribosome-bound or released form with only a slight increase in the amount of the four-glycan species observed upon release (Figure 2B, lanes 9 and 12). Thus, puromycin-dependent changes in CRT binding to the 153-mer would be attributed to the release into the lumen. Similar to the 128-mer, the puromycin-released 153-mer showed a strong increase in CRT binding (Figure 6C, lanes 7–12). We conclude that release of the HA protein from the translocon into the lumen increases accessibility of the nascent HA chains to CRT and, hence, increased its binding. These data show that the topography of the translocation machinery at the translocon dictates when soluble lumenal chaperones can access nascent chains.

Disulfide Bond Formation Commences When the First Native Disulfide Pair Emerges into the Lumen

Disulfide bond formation within HA has been shown to begin cotranslationally (Chen et al., 1995). However, the point at which disulfide bond formation commences is unknown, since the shortest HA chains could not be visualized with this assay that relied primarily upon the formation of large disulfide loops. To investigate when HA oxidation begins, nascent chains of various lengths were translated under oxidizing conditions and resolved by nonreducing and reducing SDS-PAGE. Generally, covalent intramolecular disulfide bonds result in a more compact structure that migrates faster on nonreducing SDS-PAGE.

The 107- and 128-mers showed no difference in mobility on reducing versus nonreducing SDS-PAGE (Figure 6D, lanes 4–7). The first increase in mobility on nonreducing SDS-PAGE was observed with the 153-mer (Figure 6D), the shortest construct that had both Cys residues of a native disulfide bond (Cys64-76) positioned within the ER lumen. Thus, disulfide bond formation initiated after Cys76 entered the ER lumen and was accessible to lumenal proteins.

Discussion

Our findings have been assembled into a detailed model that describes the cotranslational maturation of HA in the ER (Figure 7). The model indicates that glycans direct many of the interactions that assist and protect the nascent chain during the early stages of maturation. This involves delaying the folding of the distal portion of a nonsequential folding domain of HA until its partner is synthesized and translocated into the lumen. It also appears to involve, as discussed below, the positioning of

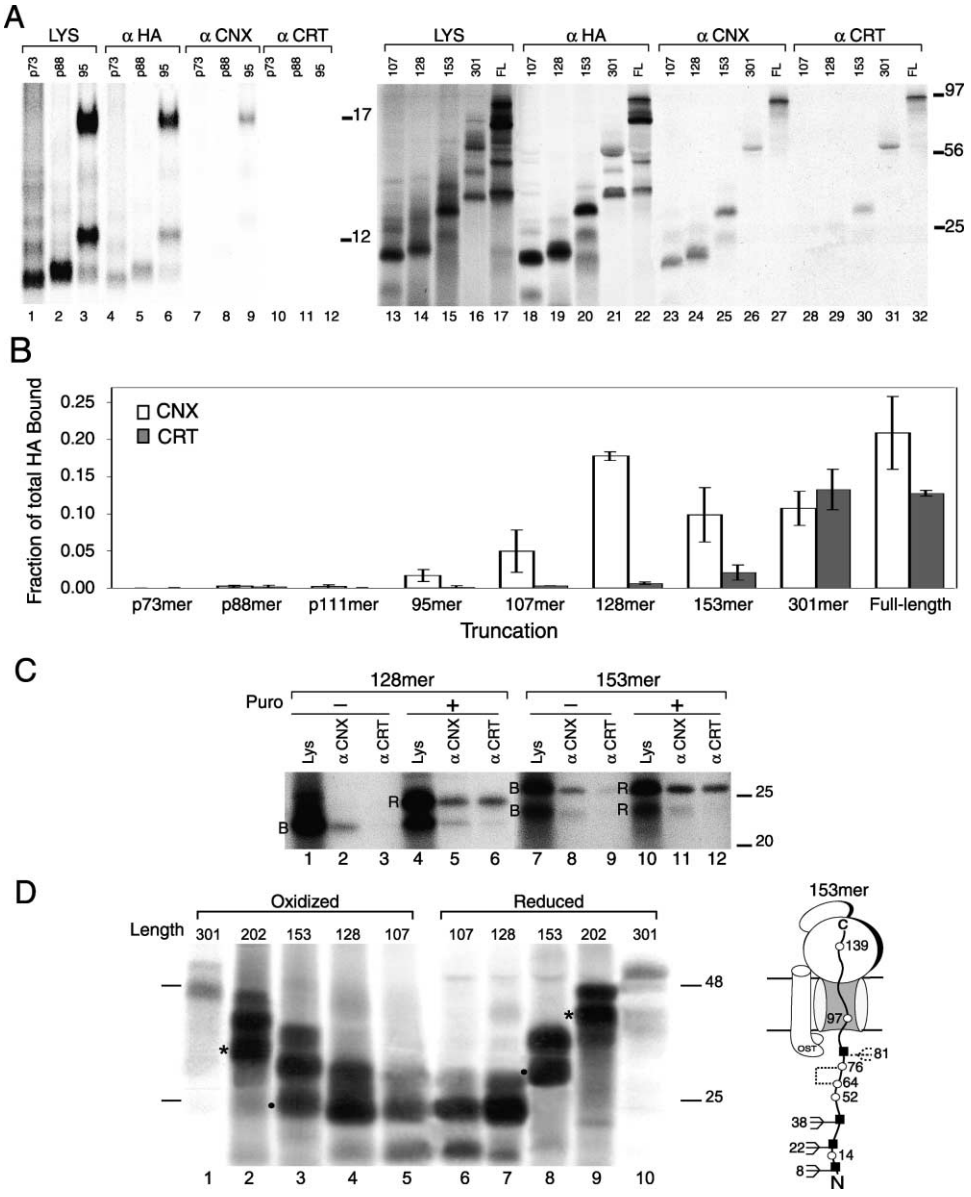

Figure 6. CNX and CRT Binding and HA Disulfide Bond Formation Are Dependent on the Nascent Chain Length and Location within the ER

(A) HA chains of different lengths were translated. Translation products were examined directly (lanes 1–3 and 13–17), immunoprecipitated with HA antisera (lanes 4–6 and 18–22), or coimmunoprecipitated with anti-CNX (lanes 7–9 and 23–27) or anti-CRT antisera (lanes 10–12 and 28–32). Samples 1–12 and 13–32 were analyzed by 14% Tris-tricine-PAGE and a 5%–20% SDS-PAGE, respectively.

(B) The fraction of HA polypeptide bound to CNX and CRT was determined by immunoprecipitation. Chaperone binding from three independent experiments was quantified using Image Quant 1.2 software.

(C) CNX and CRT binding is glycan and location dependent. The 128- and 153-mers were translated and then released with puromycin and examined directly ("Lys") or after coimmunoprecipitation with CNX or CRT antisera. HA ribosome-bound ("B") and -released ("R") chains are indicated.

(D) Disulfide bond formation begins when the first native disulfide pair emerges into the lumen. ^{35}S-labeled HA nascent chains were translated and immunoprecipitated with HA antisera prior to analysis on 7.5%–12.5% SDS-PAGE under reducing or nonreducing conditions.

glycans near Cys residues to minimize improper and premature disulfide bond formation. Indeed, our results are consistent with glycans playing an active role in controlling nascent chain processing and suggest that specific glycosylation sites have evolved in the protein to regulate its maturation.

Initially, the hydrophobic N-terminal signal sequence of HA targets the ribosome-nascent chain complex to the ER membrane in an SRP-dependent manner and then tethers the N terminus of the nascent chain to the membrane prior to its cleavage. Upon signal sequence cleavage (step 3), the two N-terminal glycans are efficiently transferred and trimmed, leading to CNX binding. As elongation continues, additional glycans are added to the top domain of HA that extends into the lumen, and they are bound by soluble CRT (step 5). Oxidation

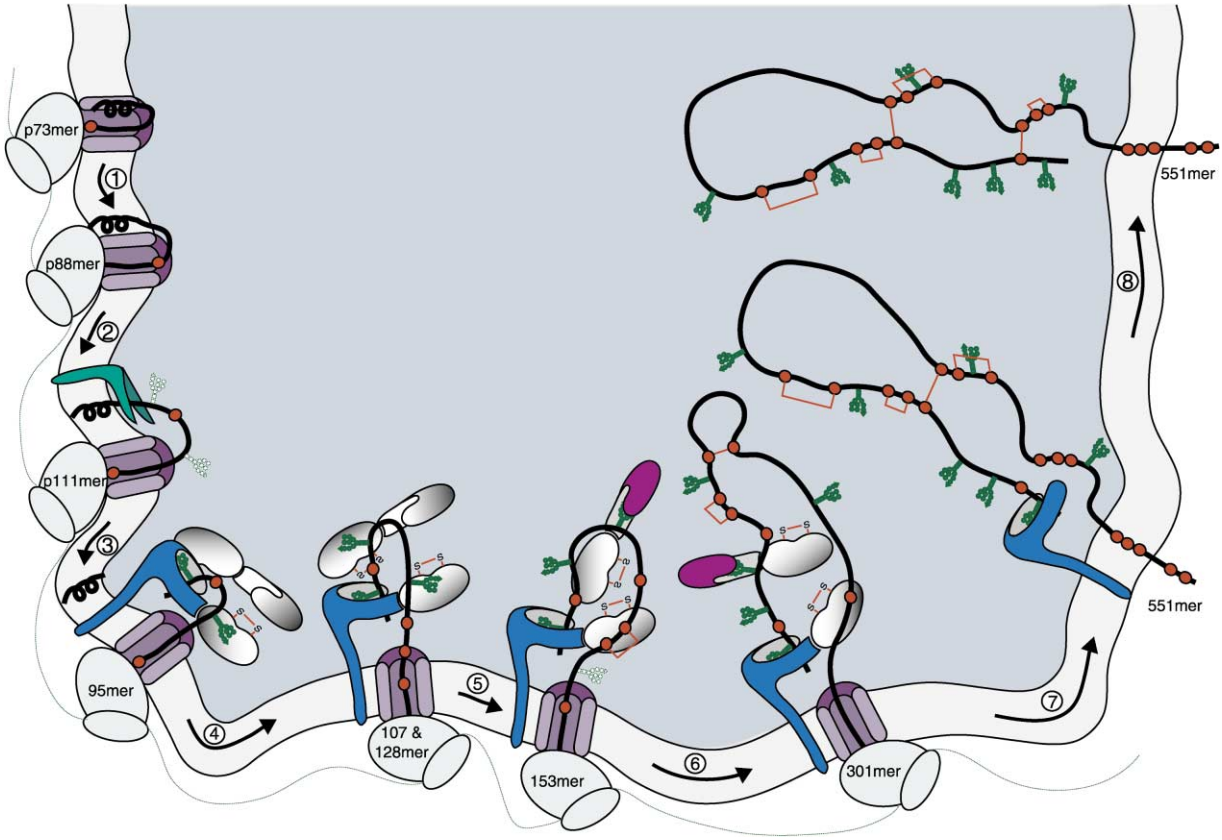

Figure 7. Model of the Cotranslational Maturation of HA

Chains are displayed docked to the ER translocon. Cys residues and disulfides are shown as filled red circles and red lines, respectively. The glycosylation state is indicated with the shaded and filled green glycans representative of partial or complete recognition, respectively. The signal sequence is depicted as a black α helix within the membrane. The cyan membrane protein is the signal peptidase complex. CNX and CRT are shown in blue and purple, respectively, when interacting with HA through its lectin domains. CRT and ERp57 that are crosslinkable but unbound by native immunoprecipitations are depicted in the shaded form.

and folding begin in the top domain, resulting in the release of CRT (steps 6 and 7), while CNX binding persists until the C terminus is available for interactions with the N terminus and the assembly of the membrane-proximal stem domain.

The proximity of the mature N terminus of HA to the membrane led to the proposal that the signal sequence assists in the early stages of folding by anchoring the N-terminal region in its native position upon entry into the ER lumen (Wilson et al., 1981). Using two independent methods, we have shown that the signal sequence of HA is removed early, after the translation of 111 amino acids (including the 16 residue signal sequence). This indicates that the nascent chain is localized at the membrane for only a short time via the signal sequence.

Prior to signal sequence cleavage, the glycans at Asn8 and 22 on the p111-mer are partially glycosylated, creating either an unglycosylated or monoglycosylated chain. The inefficient recognition of Asn8 and 22 is likely due to the restricted movement of the N terminus while the signal sequence is attached. The signal sequence anchors Asn8 too close to the membrane and positions Asn22 on an extended loop only $\sim$12 residues into the lumen. Both positions are suboptimal for OST recognition. The first phenomenon has been previously observed in yeast (Chen et al., 2001). Subsequent cleavage of the signal sequence liberates the N terminus from the membrane, initiating a cascade of events including glycan addition to Asn8 and 22 on the newly generated 95-mer and chaperone binding (step 3).

Our results paint a more complete picture than previously available for the roles of carbohydrates in directing the molecular choreography of a maturing nascent chain. The addition of N-linked carbohydrates involves the covalent attachment of a 30 Å $\times$ 10 Å $\times$ 10 Å hydrophilic structure to the polypeptide (Rudd et al., 2001). Not only does this modification dramatically decrease the hydrophobicity of the polypeptide, it also provides binding sites for the lectin chaperones CNX and CRT, recruiting ERp57 in the process. Each of these properties has a major impact on the folding reaction, because the flexible glycans can recruit chaperones to defined sites on the nascent chain, and the hydrophilic nature of the glycan ensures that their location remains largely aqueous accessible. For instance, CNX binding to the N terminus provides a longer-lasting attachment and likely a higher degree of flexibility than signal sequence insertion in the membrane. Here, membrane-bound CNX was first observed to bind the N-terminal glycans of HA immediately after signal sequence cleavage, providing

a mechanism to confine the N terminus close to the membrane surface.

Chemical crosslinking to Cys14 in the 95-mer demonstrated that CRT and the oxidoreductase ERp57 are in the vicinity of the translocon immediately after signal sequence cleavage (Figures 4 and 5A). Crosslinking of HA to CRT and ERp57 was dependent on the presence of trimmed N-linked glycans. However, the efficient binding of CRT (as determined by coimmunoprecipitation) to carbohydrates was observed after the top domain glycan at Asn81 was attached to the 153-mer (Figures 6A and 6B, 153-mer, and Figure 7, colored CRT). Since CRT binding was observed at a later point than crosslinking by CRT, CRT apparently requires two or more glycans to survive the coimmunoprecipitation procedure, with perhaps a single glycan being sufficient for recruitment and crosslinking. This requirement was observed previously with RNaseB (Rodan et al., 1996).

The recently solved crystal structure of the lumenal domain of CNX provides an explanation for our chemical crosslinking results (Schrag et al., 2001). Crosslinking with BMH efficiently trapped interactions between HA and CRT/ERp57, but crosslinking of HA to CNX was not observed. Mature CNX possesses a single free Cys (Cys442) situated on the opposite face of the CNX lectin binding domain, where its accessibility to a CNX-bound substrate would be poor. In contrast, the soluble CRT contains a lone free Cys (Cys163) that is located between the lectin binding domain and the extended hairpin arm of the P domain, placing it in an optimal location for crosslinking to substrates by BMH. Thus, the inability to crosslink HA to CNX likely results from a suboptimal arrangement of Cys residues on CNX.

HA binding to soluble CRT dramatically increased after glycans were attached at positions 165 and 285. This finding implicates the top domain glycans in CRT binding (Figures 6A and 6B, 301-mer, and Figure 7, step 5), supporting the observation that CRT bound only the early oxidative intermediates of full-length HA (Hebert et al., 1996; and data not shown). Folding of HA starts at the top of the protein and progresses toward the membrane, as demonstrated by the binding of conformation-specific antibodies and by the sequence of disulfide bond formation (Braakman et al., 1992). Therefore, once the globular domain has folded, its glycans would no longer be reglucosylated by UGT, permitting the early release of CRT. This regional recognition of misfolded domains by purified UGT has previously been shown using a chimeric protein substrate in vitro (Ritter and Helenius, 2000). These results indicate that UGT works locally within folding domains by modifying the malfolded or incompletely folded region, thereby recruiting chaperones only to the nonnative domains of a protein.

Ablation of CNX and CRT binding to HA by pretreatment with glucosidase inhibitors reduced the fraction of HA that reached its correctly folded and assembled state and increased the extent of aggregation. Furthermore, when the release of HA from the chaperones was inhibited by the posttranslational addition of glucosidase inhibitors, HA folding and oligomerization were arrested (Hebert et al., 1996). Together, these results suggest that folding and oxidation occur after the substrate is released by the lectin chaperones. Thus, CNX and CRT binding promote the efficient folding and assembly of proteins by slowing the folding and oligomerization processes (Hebert et al., 1996; Vassilakos et al., 1996). The fidelity of the maturation processes appears to be increased by a decrease in rate. CNX and CRT binding to HA presumably functions to shield the top domain (CRT) and the stem domain (CNX) from nonproductive aggregation-prone interactions.

For proteins consisting of a series of individual folding domains, cotranslational folding provides a mechanism to separate the folding of domains both spatially and temporally. However, proteins such as HA require the joining of distal sites for efficient folding. Its folding may require a mechanism to inhibit the folding of the N-terminal portion of the distal folding domain while its C-terminal partner is being translated. The localization of multiple glycans at the N terminus of HA appears to perform this function by ensuring nascent chain interaction with lectin chaperones. The importance of these glycans is emphasized by the fact that three of the seven glycans on HA are found here and that these N-terminal glycans are conserved in various *influenza* strains.

The potential roles of CNX binding to the N-terminal HA glycans are 3-fold. First, CNX binding to the N terminus of the protein retains it proximal to the membrane after signal sequence cleavage. Second, the three glycans at Asn8, 22, and 38 surround the critical Cys14 that is involved in the large disulfide loop that joins the N- and C termini together. Since Cys14 is the first Cys to enter the lumen during translation, it must be protected from forming nonnative intramolecular disulfides until its disulfide partner appears at Cys466, 9 Cys and 8 min of translation later. The retention and protection of the N terminus of HA by CNX binding to these glycans is supported by previous work showing the removal of these three glycans by mutagenesis accelerated the co- and posttranslational folding of HA with an overall decrease in efficiency (Hebert et al., 1997). Finally, since CNX is associated with oxidoreductase ERp57 (Oliver et al., 1999), CNX binding to this site recruits ERp57. ERp57 can then act as an electron acceptor to catalyze the oxidation reaction once the disulfide partners have emerged, or as an electron donor to assist in disulfide bond rearrangement. Therefore, CNX binding to the N-terminal glycans, and similarly CRT binding to the globular glycans, causes a delay in the folding of HA, orchestrating the concerted oxidation of HA that occurs upon release from the lectin chaperones.

Since Cys residues form covalent disulfide bonds within the oxidizing conditions of the ER, they can be vulnerable residues for protein folding. However, it appears improper disulfide bond formation can be minimized by the ability of a nearby glycan to recruit the lectin chaperones and thereby block improper Cys-Cys reactions. In this way, a lone Cys can be protected from reacting covalently with other Cys residues in the protein. Similarly, a Cys involved in an intermolecular disulfide may be protected by a nearby glycan until the monomers have folded into their native conformations and are ready for posttranslational disulfide bond formation. Also, as discussed above, the N-terminal Cys of a large loop disulfide pair may be protected by binding a nearby glycan to a lectin chaperone (e.g., HA to CNX) until its disulfide partner appears. In addition, the direct interac-

tion between lectin chaperones and ERp57 suggests a fourth potential mechanism whereby glycans can recruit ERp57 to a particular region to assist in the oxidation or disulfide rearrangement of a protein.

Here, we have proposed a highly detailed model for the folding of a glycoprotein in its natural environment. The data indicate that N-linked glycans can direct the molecular choreography for a ribosome-bound nascent chain as it emerges from the translocon by mediating interactions with chaperones and a foldase, ERp57. Anfinsen's seminal studies indicated that the primary sequence of a protein possessed all the information required for it to obtain its native structure (Anfinsen, 1973). Years later, we find an additional level of complexity programmed into the primary sequences of proteins. Specifically, N-linked glycans can be positioned to facilitate the efficient acquisition of native protein structure in the cell. This may be especially true for viral proteins that evolve more rapidly than host cellular proteins and have developed methods to evade immune detection. Not only can N-linked carbohydrates mask antigenic epitopes by sterically disrupting antibody recognition (Reitter et al., 1998), they can also mediate the recruitment of chaperones to ensure the folding reaction is optimized and degradation (or production of immunogenic peptides) is minimized. Therefore, N-linked glycans constitute a very complex, but important role in directing the mechanism of glycoprotein maturation in the cell. Further experimentation is required to determine the scope of the substrates that are assisted by glycans and to test the potential mechanisms that use glycans to direct their maturation.

Experimental Procedures

Reagents

RNasin and components of the reticulocyte cell-free translation systems were purchased from Promega (Madison, WI). Canine pancreas microsomes and ERp57 antiserum were gifts from Dr. R. Gilmore (Worcester, MA) and Dr. T. Wileman (Woking, UK), respectively. EasyTag express ^{35}S-labeling mix and Zysorbin were obtained from PerkinElmer (Boston, MA) and Zymed Laboratories (San Francisco, CA), respectively. CNX and HA antisera were from Dr. A. Helenius (Zurich). CRT (PA3-900) antiserum, T7 expression system, and bismaleimidohexane (BMH) were purchased from Affinity BioReagents (Golden, CO), Ambion (Austin, TX), and Pierce (Rockford, IL). All other chemicals were from Sigma Chemical (St. Louis, MO).

Construction of HA Mutants and mRNA Transcription

Mutations to the HA cDNA in pBluescript were created using Stratagene's mutagenesis kit (La Jolla, CA). The Met-enhanced signal sequence construct (HA-SS^{MM}) was produced by changing the amino acids −14 (Thr) and −12 (Ile) in the sequence to Met. Three Met-enhanced constructs were made for the six shortest nascent chains. For the p73-, p88-, and p111-mers, the amino acids 42–44 and 50–52 in the mature protein were changed to Met-Met-Met. In the 107- and 128-mers, the amino acids 87–89 and 100–102 were altered, while the 153-mers had the amino acid residues 100–102 and 136–138 mutated. All mutations were verified by DNA sequencing.

All of the HA cDNA constructs were linearized with KpnI to produce the full-length 551-mer and NdeI, HincII, PshaI, EcoNI, AlwNI, Eco 0109, and BsgI to produce the 301-mer, 153-mer, 128-mer, 107-mer, 95-mer/p111-mer, p88-mer, and p73-mer truncations, respectively. The linearized cDNAs were transcribed with Ambion's T7 expression system.

Translations

Full-length and truncated HA proteins were translated and translocated into canine pancreas microsomes at 27°C for 30 min as described previously (Hebert et al., 1995), using 1 mM DTT and 4 mM GSSG when oxidizing conditions were required. When [^{35}S]Met was used as a label, the translation mixture included 22 μM Cys. To initiate ribosomal release, 1 mM puromycin was added to the translation mixture and incubated at 27°C for 10 min. After translation, samples were alkylated with 20 mM NEM on ice to block free sulfhydryls (Braakman et al., 1992).

Crosslinking

For crosslinking experiments, NEM was not added after translation. For samples treated with the glycosylation inhibitors, the translation mix was preincubated with either 1 mM DNJ or 2 mM NYT for 10 min at 27°C before the addition of mRNA. Translations were stopped on ice for 10 min with 1 mM cycloheximide prior to isolating ^{35}S-labeled HA-ribosome-microsome complexes by ultracentrifugation through an isotonic sucrose cushion (250 mM sucrose, 500 mM KOAc, 5 mM $Mg(OAc)_2$, and 50 mM HEPES-KOH [pH 7.9]) for 10 min at 157,000 × g at 4°C. Microsomes were resuspended in a buffer (250 mM sucrose, 100 mM KOAc, 5 mM $Mg(OAc)_2$, and 50 mM HEPES-KOH [pH 7.9]). Crosslinking with 0.8 mM BMH was performed at 27°C for 10 min then quenched by the addition of 0.1 volumes of 100 mM β-mercaptoethanol (Oliver et al., 1999).

PNGase F Digestion, CTAB Precipitations, and Immunoprecipitations

PNGase F digestions were carried out as described previously (Ujvari et al., 2001). Anti-HA immunoprecipitations were also performed as described previously (Hebert et al., 1995). For anti-CNX, CRT, or ERp57 immunoprecipitations, alkylated samples were solubilized in 2% (w/v) CHAPS in HBS (50 mM HEPES and 200 mM NaCl [pH 7.5]) and were rotated with Zysorbin for 1 hr at 4°C. Anti-Sec61α and anti-TRAM immunoprecipitations were performed as described in Do et al. (1996). For denaturing immunoprecipitations, the samples were treated with 1% (w/v) SDS and heated to 95°C for 5 min prior to lysis. After rotation, the samples were centrifuged for 5 min at 10,000 × g at 4°C. 100 μl of 10% (v/v) protein A-Sepharose beads, and CNX, CRT, or ERp57 antiserum were added to the supernatant. The samples were then rotated for 12 hr at 4°C. Immune complexes were centrifuged for 5 min at 5250 × g at 4°C. For anti-CNX, anti-CRT, or anti-ERp57 precipitations, pellets were washed once with 0.5% (w/v) CHAPS, or once with Sec or TRAM buffer for anti-Sec61α and TRAM precipitations, respectively. Ribosome-bound chains were precipitated with CTAB according to Gilmore et al. (1991) after isolation of the microsome-containing ^{35}S-labeled HA by ultracentrifugation as described above. Where indicated, samples were divided into two equal aliquots, and 0.1 M DTT was added to the reducing samples prior to resolution by SDS-PAGE. ^{35}S-HA levels were quantified with a Storm 840 phosphorimager from Molecular Dynamics (Sunnyvale, CA) and Image Quant 1.2 software.

Acknowledgments

We are indebted to Dr. Ari Helenius (Zurich) for the gift of antibodies and valuable advice. We also thank Dr. Lila Gierasch for critical reading of the manuscript. R.D. was supported by a Chemistry-Biology Interface Training grant from the N.I.H. This work was supported by grants from the N.I.H. to D.N.H. and A.E.J., and The Robert A. Welch Foundation (A.E.J.).

Received: September 3, 2002
Revised: October 25, 2002

References

Anfinsen, C.B. (1973). Principles that govern the folding of protein chains. Science *181*, 223–230.

Braakman, I., Helenius, J., and Helenius, A. (1992). Manipulating disulfide bond formation and protein folding in the endoplasmic reticulum. EMBO J. *11*, 1717–1722.

Chen, W., and Helenius, A. (2000). Role of ribosome and translocon

complex during folding of influenza hemagglutinin in the endoplasmic reticulum of living cells. Mol. Biol. Cell *11*, 765–772.

Chen, W., Helenius, J., Braakman, I., and Helenius, A. (1995). Cotranslational folding and calnexin binding of influenza hemagglutinin in the endoplasmic reticulum. Proc. Natl. Acad. Sci. USA *92*, 6229–6233.

Chen, X., VanValkenburgh, C., Liang, H., Fang, H., and Green, N. (2001). Signal peptidase and oligosaccharyltransferase interact in a sequential and dependent manner within the endoplasmic reticulum. J. Biol. Chem. *276*, 2411–2416.

Do, H., Falcone, D., Lin, J., Andrews, D.W., and Johnson, A.E. (1996). The cotranslational integration of membrane proteins into the phospholipid bilayer is a multistep process. Cell *85*, 369–378.

Ellgaard, L., Molinari, M., and Helenius, A. (1999). Setting the standards: quality control in the secretory pathway. Science *286*, 1882–1888.

Frydman, J., Erdjument-Bromage, H., Tempst, P., and Hartl, F.U. (1999). Co-translational domain folding as the structural basis for the rapid de novo folding of firefly luciferase. Nat. Struct. Biol. *6*, 697–705.

Gilmore, R., and Blobel, G. (1985). Translocation of secretory proteins across the microsomal membrane occurs through an environment accessible to aqueous perturbants. Cell *42*, 497–505.

Gilmore, R., Collins, P., Johnson, J., Kellaris, K., and Rapiejko, P. (1991). Transcription of full-length and truncated mRNA transcripts to study protein translocation across the endoplasmic reticulum. Methods Cell Biol. *34*, 223–239.

Hammond, C., Braakman, I., and Helenius, A. (1994). Role of N-linked oligosaccharides, glucose trimming and calnexin during glycoprotein folding in the endoplasmic reticulum. Proc. Natl. Acad. Sci. USA *91*, 913–917.

Hardesty, B., Tsalkova, T., and Kramer, G. (1999). Co-translational folding. Curr. Opin. Struct. Biol. *9*, 111–114.

Hebert, D.N., Foellmer, B., and Helenius, A. (1995). Glucose trimming and reglucosylation determines glycoprotein association with calnexin. Cell *81*, 425–433.

Hebert, D.N., Foellmer, B., and Helenius, A. (1996). Calnexin and calreticulin promote folding, delay oligomerization and suppress degradation of influenza hemagglutinin in microsomes. EMBO J. *15*, 2961–2968.

Hebert, D.N., Zhang, J.-X., Chen, W., Foellmer, B., and Helenius, A. (1997). The number and location of glycans on influenza hemagglutinin determine folding and association with calnexin and calreticulin. J. Cell Biol. *139*, 613–623.

Helenius, A. (1994). How N-linked oligosaccharides affect glycoprotein folding in the endoplasmic reticulum. Mol. Biol. Cell *5*, 253–265.

Krieg, U.C., Johnson, A.E., and Walter, P. (1989). Protein translocation across the endoplasmic reticulum membrane: identification by photocross-linking of a 39-kD integral membrane glycoprotein as part of a putative translocation tunnel. J. Cell Biol. *109*, 2033–2043.

Molinari, M., and Helenius, A. (1999). Glycoproteins form mixed disulphides with oxidoreductases during folding in living cells. Nature *402*, 90–93.

Netzer, W.J., and Hartl, F.U. (1997). Recombination of protein domains facilitated by co-translational folding in eukaryotes. Nature *388*, 343–349.

Nicola, A.V., Chen, W., and Helenius, A. (1999). Co-translational folding of an alphavirus capsid protein in the cytosol of living cells. Nat. Cell Biol. *1*, 341–345.

Oliver, J.D., Roderick, H.L., Llewellyn, D.H., and High, S. (1999). ERp57 functions as a subunit of specific complexes formed with the ER lectins calreticulin and calnexin. Mol. Biol. Cell *10*, 2573–2582.

Reitter, J.N., Means, R.E., and Desrosiers, R.C. (1998). A role for carbohydrates in immune evasion in AIDS. Nat. Med. *4*, 679–684.

Ritter, C., and Helenius, A. (2000). Recognition of local glycoprotein misfolding by the ER folding sensor UDP-glucose:glycoprotein glucosyltransferase. Nat. Struct. Biol. *7*, 278–280.

Rodan, A.R., Simons, J.F., Trombetta, E.S., and Helenius, A. (1996). N-linked oligosaccharides are necessary and sufficient for association of RNase B with calnexin and calreticulin. EMBO J. *15*, 6921–6930.

Rudd, P.M., Elliott, T., Cresswell, P., Wilson, I.A., and Dwek, R.A. (2001). Glycosylation and the immune system. Science *291*, 2370–2376.

Schrag, J.D., Bergeron, J.J.M., Li, Y., Borisova, S., Hahn, M., Thomas, D.Y., and Cygler, M. (2001). The structure of calnexin, an ER chaperone involved in quality control of protein folding. Mol. Cell *8*, 633–644.

Sousa, M., and Parodi, A.J. (1995). The molecular basis for the recognition of misfolded glycoproteins by the UDP-Glc:glycoprotein glucosyltransferase. EMBO J. *14*, 4196–4203.

Ujvari, A., Aron, R., Eisenhaure, T., Cheng, E., Parag, H.A., Smicun, Y., Halaban, R., and Hebert, D.N. (2001). Translation rate of human tyrosinase determines its N-linked glycosylation level. J. Biol. Chem. *276*, 5924–5931.

Vassilakos, A., Cohen-Doyle, M.F., Peterson, P.A., Jackson, M.R., and Williams, D.B. (1996). The molecular chaperone calnexin facilitates folding and assembly of class I histocompatibility molecules. EMBO J. *15*, 1495–1506.

Whitley, P., Nilsson, I., and von Heijne, G. (1996). A nascent secretory protein may traverse the ribosome/endoplasmic reticulum translocase complex as an extended chain. J. Biol. Chem. *271*, 6241–6244.

Wilson, I.A., Skehel, J.J., and Wiley, D.C. (1981). Structure of the haemagglutinin membrane glycoprotein of influenza virus at 3 Å resolution. Nature *289*, 366–373.

Zapun, A., Darby, N.J., Tessier, D.C., Michalak, M., Bergeron, J.J., and Thomas, D.Y. (1998). Enhanced catalysis of ribonuclease B folding by the interaction of calnexin or calreticulin with ERp57. J. Biol. Chem. *273*, 6009–6012.